

1 This document is the Accepted Manuscript version of a Published Work that appeared in final form in [JournalTitle], copyright ©
2 American Chemical Society after peer review and technical editing by the publisher. To access the final edited and published
3 work see <https://pubs.acs.org/doi/abs/10.1021/acs.est.9b06526>
4
5
6

7 **Effects of Sunlight on the Formation Potential of Dichloroacetonitrile and** 8 **Bromochloroacetonitrile from Wastewater Effluents**

9
10
11

12 Jiale Xu, Zachary T. Kralles, Christine H. Hart, Ning Dai*

13
14
15
16

17 Department of Civil, Structural and Environmental Engineering
18 University at Buffalo, The State University of New York, Buffalo, NY, 14260
19
20
21
22
23

24 *Corresponding author: Post address: 231 Jarvis Hall, Buffalo, NY 14260

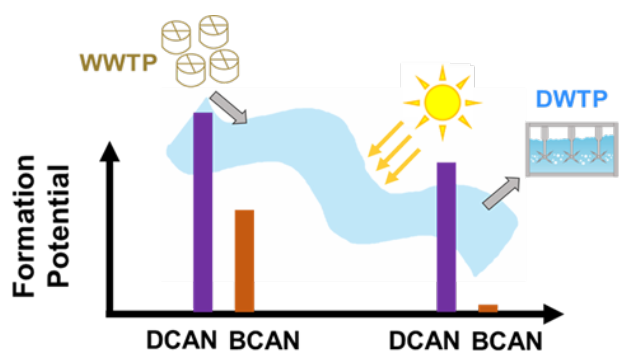
25 Phone: (716) 645-4015; Fax: (716) 645-3667

26 Email: ningdai@buffalo.edu

Abstract

Sunlight plays an important role in transforming effluent organic matter as wastewater effluents travel downstream, but the corresponding effects on the formation of haloacetonitriles (HANs), a group of toxic disinfection byproducts, in wastewater-impacted surface water has not been thoroughly investigated. In this study, we observed that sunlight preferentially attenuated the formation potential of bromochloroacetonitrile (BCAN-FP) over that of dichloroacetonitrile (DCAN-FP) in chlorine- and UV-disinfected secondary effluents. For four effluent samples from different plants, 36 h irradiation by simulated sunlight removed 28%–33% of DCAN-FP and 41%–48% of BCAN-FP. Across a larger set of effluent samples ($n = 18$), 8 h irradiation (equivalent to 2–3 d of natural sunlight) decreased the calculated cytotoxicity contributed by dihaloacetonitrile-FP in most samples. Similar behavior was observed for a mixture of wastewater and surface water (volume ratio 1:1). For UV-disinfected effluents, the higher the UV dose, the more likely was there a reduction in DCAN-FP and BCAN-FP in the subsequent sunlight irradiation. Experiments with model compounds showed that fulvic acid and UV photoproducts of tryptophan yield excited triplet state organic matters during sunlight irradiation and play an important role in promoting the attenuation of HAN precursors.

43 **Graphical abstract**



44

1. Introduction

Haloacetonitriles (HANs) are a group of nitrogenous disinfection byproducts (N-DBPs) widely detected in drinking water and disinfected wastewater effluents.^{1, 2} Toxicity assays using mammalian cells showed that they exhibit 10–1000 times higher cytotoxicity and genotoxicity than the trihalomethanes currently regulated by the U.S. Environmental Protection Agency (EPA).³ A national survey of U.S. drinking water in the late 1990s reported HAN concentrations ranging from 0.8 to 8.2 µg/L (25th and 90th percentile) in plant effluents; it also showed that dichloroacetonitrile (DCAN) and bromochloroacetonitrile (BCAN) are the two most prevalent species, with a median concentration at 1.3 and 0.7 µg/L, respectively.¹ After integrating the concentration and toxicity of individual DBPs in drinking water, HANs emerge as the most harmful DBP group, contributing to 45–83% of the overall toxicity, more than any of the other 10 known DBP groups.⁴

Recently, the concern of HAN increased along with the increase of wastewater impacts on source waters.^{5, 6} A case study on a U.S. watershed highly impacted by wastewater effluents showed that the formation potential of HANs was 3–4 times higher in samples collected downstream of three wastewater treatment plants (WWTPs) than those collected upstream.⁶ Another case study in Thailand also reported that the average HAN formation potential of wastewater effluents was 1.1–2.5 times higher than that of the corresponding upstream river waters.⁵ HAN formation positively correlates with the concentration of dissolved organic nitrogen (DON),⁶⁻⁸ which has 6 times higher average concentration in wastewater effluent than in pristine surface water.⁹ Nitrogenous organic compounds such as free amino acids^{10, 11} and nucleic acids¹⁰ can form DCAN at yields ranging from <0.05% to 1.5% by chlorination. Bromide ion, which is more abundant in wastewater (median concentration 0.19 mg/L²) than in surface water (median

concentration 35 $\mu\text{g/L}$ ¹²), can also promote HAN formation.⁷ Specifically, the formation of brominated HANs is greatly enhanced by the presence of bromide, as shown in solutions containing model precursors such as tryptophan¹³ and natural organic matter¹⁴ as well as in authentic drinking waters¹⁵ and wastewater¹⁶ samples.

Sunlight plays an important role in transforming effluent organic matter, as suggested by the decreases in ultraviolet (UV) absorbance, fluorescence intensity, and/or DON concentration.¹⁷⁻²³ Our recent work also showed that sunlight can attenuate the formation potential of trichloronitromethane (TCNM-FP) for non-nitrified wastewater effluents; in the presence of nitrite, however, TCNM-FP can increase by up to 3.6 $\mu\text{g/mg C}$, potentially attributed to the formation of nitrated precursors under sunlight.²⁴ To date, only a few studies investigated the sunlight effects on the HAN formation potential (HAN-FP) of wastewater effluents.^{25,26} One study reported a 47% reduction in DCAN-FP for two wastewater effluents after 13 h sunlight irradiation,²⁵ however, both samples were from nitrified-denitrified and UV-disinfected effluents, which may not represent other types of effluents. Another study reported a 17% reduction in DCAN-FP for the supernatant of an activated sludge-seeded aerobic microcosm after 48 h irradiation.²⁶ BCAN formation was either below detection limit or not analyzed in these two studies, but other studies have shown that the BCAN-FP of wastewater effluents can be comparable to their DCAN-FP.^{27,}

²⁸

The composition and photo-reactivity of effluent organic matter are influenced by nitrification² and wastewater disinfection^{29,30}, but the behavior of different wastewater effluents under sunlight has not been considered. A survey of 23 U.S. WWTPs reported that well-nitrified effluents had 1.4 times higher specific UV absorbance at 254 nm (SUVA) than non-nitrified effluents, but 50% lower DON concentration.² Chlorination disinfection decreased the

fluorescence signals corresponding to tryptophan- and tyrosine-like moieties more than those corresponding to humic-like moieties, while UV disinfection decreased the fluorescence intensity of the three moieties similarly.³⁰

The aim of this study was to examine the effects of sunlight on the potential of wastewater effluents to form HANs. We collected secondary effluent samples, simulated wastewater disinfection in the laboratory by chlorine or UV, irradiated the samples under simulated sunlight, and then measured the HAN-FP of the irradiated samples and compared it with the non-irradiated samples. Similar experiments were conducted on a mixture of pristine surface water and wastewater effluent. For UV-disinfected effluents, the effect of UV disinfection fluence on the extent of HAN-FP attenuation in the subsequent sunlight irradiation was evaluated. To provide mechanistic insight, we evaluated the effects of sunlight on the HAN-FP of model precursors that exhibit sunlight reactivity and correlations with wastewater HAN-FP, and identified the key components in wastewater effluents that contribute to their observed behavior under sunlight.

2. Materials and Methods

2.1. Materials

Detailed information about the chemicals used in this study is shown in Text S1.

2.2. Wastewater and Surface Water Sampling

Secondary effluents from four WWTPs were collected before disinfection and shipped to the laboratory on ice within 2 h. Samples from WWTPs A and B are non-nitrified effluents, while those from WWTPs C and D are nitrified effluents. Each WWTP was sampled 2–7 times over the course of 37 months. The surface water sample was the source of a drinking water treatment plant with <1% wastewater impact.³¹ Both wastewater effluent and surface water samples were filtered

immediately upon receipt by pre-combusted 0.7 μm glass fiber filters and stored at 4 °C before use. The filtered samples were used for experiments within 3 weeks after sampling. Table S1 shows the treatment process of each WWTP, sampling dates, and the water quality of each sample. Details concerning the methods and detection limits for water quality characteristics are shown in Text S2.

2.3. Wastewater Experiments

The wastewater experiments follow a three-step process: 1) simulated wastewater disinfection, 2) simulated sunlight irradiation, and 3) formation potential test (Scheme S1). Details are provided in Text S3. Briefly, the filtered secondary effluent samples were disinfected in the laboratory by sodium hypochlorite (NaOCl) or low-pressure UV to simulate wastewater disinfection. The chlorine and UV doses approximated those used in the WWTPs where samples were collected. The chlorine dose was 2 mg/L as Cl_2 with a contact time of 30 min, and residual chlorine (1–1.7 mg/L as Cl_2) was quenched by sodium thiosulfate ($\text{Na}_2\text{S}_2\text{O}_3$). The incident UV fluence was 12–150 mJ/cm^2 , of which 48%–68% was absorbed after accounting for sample absorbance at 254 nm and the path length of 2.76 cm (Table S2). Simulated sunlight irradiation was carried out in a Q-SUN Xe-1 test chamber (Q-Lab Corporation, Westlake, OH; intensity is shown in Figure S1) in quartz disc-covered crystallization dishes. The light intensity was 320 W/m^2 as determined by the 2-nitrobenzaldehyde chemical actinometry.³² Sample temperature was maintained at 20 °C using a circulating water bath. Most samples were irradiated for 8 h, but one or two samples from each treatment plant (randomly selected) were irradiated for 4–36 h. The formation potential (FP) test followed a similar procedure developed by Krasner et al.² for surveying the HAN-FP of wastewater effluents, with the exception that longer contact time (72 instead of 24 h) was used. A similar procedure was also used in previous studies on the sunlight

effects on DCAN-FP.^{25, 26} Sample solutions were buffered at pH 7.2 with 10 mM phosphate buffer, and then spiked with NaOCl to achieve a chlorine dose of $\text{NaOCl (mg/L as Cl}_2\text{)} = 3 \times \text{DOC (mg C/L)} + 8 \times \text{NH}_3\text{-N (mg N/L)} + 10$. Four HANs, DCAN, BCAN, dibromoacetonitrile (DBAN), and trichloroacetonitrile (TCAN), were analyzed for all samples, and four trihalomethanes (THM), chloroform, dichlorobromomethane, dibromochloromethane, and bromoform were analyzed for selected samples; the method detection limit was 0.1 $\mu\text{g/L}$ for each DBP. DBPs were also analyzed after the simulated wastewater disinfection step (i.e., before or after sunlight irradiation; prior to FP test). Table S3 shows the values of DCAN and BCAN for chlorine-disinfected effluents. These concentrations are generally low (below detection limit to 0.2 $\mu\text{g/mg C}$), and were subtracted from the DBP concentrations after the FP test to yield the DBP-FP of the samples. For UV-disinfected effluents, DBP concentration in all samples before formation potential test was below detection limit. Details are provided in Text S3.

2.4. Excitation Emission Matrix (EEM) Analysis

Fluorescence EEM was determined using a Cary Eclipse fluorescence spectrophotometer following a published protocol.³³ Samples were diluted to a DOC concentration of 1 mg/L, spiked with KCl to achieve a concentration of 0.01 M, and then acidified to pH 3 using a 2 M HCl solution. Excitation and emission slits were set to a 10 nm band-pass. The excitation wavelength increased from 200 to 400 nm at 5 nm increments; for each excitation wavelength, emission was recorded from 290 to 550 nm at 2 nm intervals. Raw EEM data was processed to subtract blank, to correct inner-filter effect, and to remove and interpolate scatterings using an R-based parallel factor analysis (PARAFAC) model.^{34, 35} The processed EEM data was plotted in a contour plot, and the fluorescence intensity was calculated by volume integration.³⁶ EEM was divided into five regions respectively associated with tyrosine-like, tryptophan-like, fulvic acid-like, soluble microbial

product-like, and humic acid-like moieties. Figure S2 shows the EEM plot for effluent A5 as an example. The assignment of the fluorescence regions followed the recommendation from Chen et al.³⁶ We recognize that both fulvic acid and humic acid can fluoresce in region III³⁸; however, since fulvic acid is the dominant humic substance in wastewater effluent,³⁷ and its fluorescence signal is stronger than humic acid in Region III,³⁸ we used only fulvic acid to reconstruct the fluorescence signal in Region III for synthetic wastewaters (see section 3.2.2 below).

2.5. Model Precursor Experiments

To investigate the mechanisms for the observed sunlight effects on HAN-FP, experiments were conducted using solutions of model precursors, their mixtures with fulvic acid, and their mixtures with a surface water sample (SW). Four model precursors, tryptophan, tyrosine, asparagine, and Suwannee River fulvic acid, were tested. Each solution contained 5 mg C/L precursor and was buffered at pH 7.2 with 5 mM phosphate. For the mixtures with fulvic acid, 2.5 mg C/L fulvic acid was spiked into tryptophan, tyrosine, and asparagine solutions. For the mixtures with SW, a “synthetic wastewater” was first created using tryptophan (50 µg/L) and/or fulvic acid (2.5 mg C/L), and then mixed with SW. The concentrations of tryptophan and fulvic acid in the synthetic wastewater were chosen to achieve similar fluorescence signal in the corresponding regions as effluent A5 (Figure S4 and Table S4). Details are described in Text S6. The concentrations of model precursors in the “synthetic wastewater” are also similar to those measured in authentic wastewater by high performance liquid chromatography³⁹ and fractionation^{37, 40, 41} in previous studies.

Because we observed that the change in HAN-FP of UV-disinfected wastewater effluents under sunlight was influenced by the UV disinfection fluence, we quantified the overall sunlight absorption ability (290–500 nm) of selected samples. The details are shown in Text S7. To

investigate the roles of fulvic acid and tryptophan (and its UV photoproducts) in changing HAN-FP under sunlight, 2,4,6-trimethylphenol was used as a chemical probe for excited triplet state organic matters in tryptophan solutions, effluents A6 and C7, and fulvic acid solutions under sunlight, and benzoic acid was used as a chemical probe for hydroxyl radical ($\cdot\text{OH}$) in tryptophan solutions. Detailed methods are described in Text S8. The concentrations of tryptophan and its photoproducts kynurenine and tryptamine were analyzed in selected samples by liquid chromatography triple quadrupole mass spectrometer (LC-QQQ) (Text S9).

2.6. Calculation of Cytotoxicity

The total cytotoxicity contributed by dihaloacetonitrile-FP was estimated by summing the ratios of the formation potential of DCAN, BCAN, or DBAN over their corresponding LC_{50} cytotoxicity index³:

$$\text{Cytotoxicity} = \frac{\text{DCAN-FP}}{\text{LC}_{50,\text{DCAN}}} + \frac{\text{BCAN-FP}}{\text{LC}_{50,\text{BCAN}}} + \frac{\text{DBAN-FP}}{\text{LC}_{50,\text{DBAN}}} \quad (\text{Equation 1})$$

where FP (M) is the non-normalized FP of each dihaloacetonitrile, and LC_{50} (M) is the concentration of a dihaloacetonitrile that is associated with a 50% reduction in cell viability or cell growth compared to the untreated control in a Chinese hamster ovary cell assay.³ The LC_{50} index for the three chlorinated and brominated dihaloacetonitriles is shown in Table S5. TCAN was not considered in cytotoxicity calculation because of its low toxicity³ and low formation from wastewater reported in literature²⁸ and in our experiments. We recognize that HAN-FP of wastewater effluent cannot represent the HAN formation in the drinking water. Here, the calculation of cytotoxicity is used as an indicator to assess whether sunlight alters the potential toxicity of HAN formation from wastewater effluents.

3. Results and Discussion

3.1. Comparing Sunlight Effects on the DCAN-FP and BCAN-FP of Wastewater

Effluents

3.1.1. Chlorine-disinfected Wastewater Effluents

The effect of sunlight irradiation was first assessed for chlorine-disinfected wastewater effluents, because chlorination is the most common wastewater disinfection method in the U.S.⁴²,⁴³ A recent study showed that the transport time between WWTP discharge to downstream intakes ranges from less than one day to more than a week.⁴⁴ To capture a wide range of travel time, 4–36 h was employed in the experiments, roughly equivalent to 1–13 days of natural irradiation (midsummer at 40° N at sea level under clear sky; accounting for diurnal pattern).⁴⁵ Figure 1a shows that for all four effluent samples, sunlight steadily decreased both DCAN-FP and BCAN-FP, but BCAN-FP decreased faster than DCAN-FP. By the end of the 36 h irradiation, DCAN-FP decreased by 28–33%, while BCAN-FP decreased by 41–48%. Table S7 shows the fitting parameters for first-order and zero-order kinetics; first-order fitting yielded slightly higher R^2 values. The first-order rate constants for the attenuation of BCAN-FP (0.017–0.021 h⁻¹) was approximately 2-fold greater than those for DCAN-FP (0.009–0.012 h⁻¹). The concentrations of the other two HANs monitored, DBAN and TCAN, were below detection limit in most samples.

To assess whether the faster attenuation of BCAN-FP than DCAN-FP was a consistent phenomenon, each treatment plant was sampled 1 to 6 more times over the course of 37 months, yielding a total of 18 samples. All samples were irradiated for 8 h, equivalent to 2–3 days of natural irradiation. Figure 1b shows that sunlight indeed attenuated BCAN-FP to a greater extent than DCAN-FP. For DCAN-FP, two thirds of the samples had FP_{8h}/FP_0 ratios in the range 0.9–1.1 (i.e., less than 10% difference before and after irradiation). In contrast, for BCAN-FP, two thirds of the FP_{8h}/FP_0 ratios were smaller than 0.9. D1 sample exhibited unique behavior, with both DCAN-FP

and BCAN-FP increased after irradiation; the sample was collected after a heavy rainfall, so its composition may not represent typical wastewater effluents. For all samples, BCAN-FP is lower than the corresponding DCAN-FP (Table S6), but BCAN is also 7 times more cytotoxic than DCAN.³ Therefore, we calculated the total cytotoxicity contributed by all dihaloacetonitrile-FP (mostly DCAN and BCAN), and observed that 8 h sunlight irradiation reduced the overall cytotoxicity for most samples (Figure 1c).

Because the use of high chlorine dose and long contact time in FP tests amplifies DBP formation, and because the 72 h contact time used in our FP tests was longer than previous studies,^{25, 26} raising concerns for the potential HAN hydrolysis after formation,⁴⁶ we conducted FP tests on two samples using three contact times (24, 48, and 72 h). As shown in Table S8, the HAN-FP of both the nitrified and non-nitrified samples decreased with contact time in the FP test. However, the changes in DCAN-FP, BCAN-FP, and the calculated cytotoxicity by sunlight (Figure S5) were not affected by the contact times used in the FP test. Besides HANs, we also monitored the four THMs that are regulated by the U.S. EPA in our samples. As shown in Figure S6, the FP of chloroform, dichlorobromomethane, dibromochloromethane, and bromoform increased after 8 h of simulated sunlight irradiation. However, because the overall cytotoxicity contributed by both dihaloacetonitriles and THMs were dominated by dihaloacetonitriles, a net decrease in cytotoxicity was observed after sunlight irradiation (Figure S6e). Hence, the following sections will focus only on HANs alone.

Among the nine water quality parameters monitored, only specific UV absorbance at 254 nm (SUVA) exhibited changes under sunlight (Tables S10 and S11). SUVA was consistently reduced by sunlight, 5%–29% lower after 8 h irradiation and 17%–40% lower after 36 h irradiation. The attenuation rate constants of SUVA were similar to those of DCAN-FP (Figure S7a and Table

S7). A correlation was observed between the change in DCAN-FP or BCAN-FP for four effluent samples and their corresponding change in SUVA upon 36 h irradiation (Figures S7b and S7c). However, such a correlation was not observed for all effluent samples upon 8 h irradiation (Figure S8). SUVA did not correlate with DOC-normalized DCAN-FP or BCAN-FP, which contrasts previous reports that SUVA positively correlates with DOC-normalized DCAN-FP or BCAN-FP for surface waters.^{47, 48} This difference may be attributed to that the concentration of DON, as a group of HAN precursors,⁸ was reported to correlate with the aromaticity of organic matter (absorbance at 254 nm) for surface water⁴⁹ but not for wastewater effluents⁵⁰. In contrast to our recent findings that high nitrite concentrations are associated with increases in TCNM-FP after sunlight irradiation,²⁴ no relationship between nitrite concentration and the change in HAN-FP was found.

Our repeated sampling at the four WWTPs allows us to assess the variability of DCAN-FP and BCAN-FP of secondary effluents from the same WWTP (without sunlight irradiation) (Figure S9a). The ratios between the standard deviation and the mean of DCAN-FP ($n = 2-7$) for an individual WWTP were calculated to be 0.54–1.0, and those of BCAN-FP were 0.52–1.2, suggesting substantial variability among samples collected at different times. Considering that most surveys of the HAN-FP of wastewater effluents relied on 1–2 sampling at each plant,^{2, 51, 52} future surveys may consider evaluating the temporal variability. Previously, an extensive survey of U.S. secondary effluents showed that non-nitrified effluents featured higher FP of total HANs (without normalization by DOC) than nitrified effluents.⁶ In this study, FP was measured for chlorine-disinfected secondary effluents, and we also observed that non-nitrified effluents featured higher FP of DCAN and BCAN (without normalization by DOC) than nitrified effluents (Figure

S10a). After normalization by DOC, however, neither DCAN-FP nor BCAN-FP was different between non-nitrified and nitrified effluents (Figure S10b).

3.1.2. UV-disinfected Wastewater Effluents

UV is another common wastewater disinfection method. Figure 1d shows that sunlight attenuated the BCAN-FP of UV-disinfected effluents to a greater extent than their DCAN-FP, while Figure 1e shows that sunlight was able to reduce the overall cytotoxicity contributed by dihaloacetonitrile-FP for most samples. The change in DCAN-FP or BCAN-FP by sunlight was not significantly different between samples disinfected by chlorine (exposure: 30–55 mg·min/L) and UV (incident fluence: 12 mJ/cm²) (Figure S11). Previously, the DCAN-FP of two nitrified-denitrified, UV-disinfected effluents was shown to decrease under sunlight following pseudo first-order kinetics, achieving 47% reduction after 13 h irradiation (~520 W/m²).²⁵ We observed less attenuation of DCAN-FP by sunlight, presumably attributable to the light screening by nitrate (for nitrified effluents in our study) and/or the different UV fluence applied (data not available in reference²⁵). Indeed, we observed that UV disinfection fluence can influence the behavior of effluents under sunlight (see below). Nitrified and non-nitrified effluents, regardless of being disinfected by chlorine or UV, exhibited similar change in DCAN-FP and BCAN-FP under sunlight (Figure S12). Similar to that observed for chlorine-disinfected effluents, the changes in DCAN-FP, BCAN-FP, or the calculated cytotoxicity by 8 h of irradiation for UV-disinfected effluents were not affected by the contact time used in the FP test (Figure S13). Regarding HAN-FP before sunlight irradiation, UV-disinfected effluents featured higher DCAN-FP than chlorine-disinfected effluents, but their BCAN-FP was similar (Figure S14). Variability of DCAN- and BCAN-FP was also observed among UV-disinfected effluent samples collected at different times

(Figure S9b). SUVA is again the only water quality parameter changed over the course of irradiation (Table S14).

The phototransformation of dissolved organic matter is dependent on the irradiation wavelength and intensity, suggesting that UV and sunlight can play different roles on the transformation of HAN precursors. The UV incident fluence (12 mJ/cm^2) for samples shown in Figure 1d are on the low end of common doses for wastewater disinfection. Therefore, experiments were conducted on four wastewater effluent samples with varying UV disinfection fluences ($12\text{--}150 \text{ mJ/cm}^2$) prior to 8 h sunlight irradiation. Figure 2 shows that the $\text{FP}_{8 \text{ h}}/\text{FP}_0$ ratios decreased as the UV disinfection fluence increased. At low UV disinfection fluences ($<50 \text{ mJ/cm}^2$), two of the samples (B2 and D1) actually showed higher HAN-FP after sunlight irradiation. After irradiated by higher UV fluences, however, all four samples exhibited lower DCAN-FP (9%–17% lower) and BCAN-FP (19%–41% lower) after 8 h sunlight irradiation. The FP of samples before sunlight irradiation was not affected by the UV disinfection fluence (Figure S15a). We hypothesize that UV irradiation can transform HAN precursors to more sunlight susceptible forms and/or increase the reactivity of photosensitizers to degrade HAN precursors under sunlight. Indeed, we observed that effluent C6 exhibited higher sunlight absorption ability (290–500 nm) after UV disinfection; the higher the UV disinfection fluence, the greater the increase in the sunlight absorption ability (Figure S16). This is further discussed in section 3.2.3.

3.1.3. Mixture of Surface Water and Wastewater Effluent

As shown in Figure 3, the mixture of wastewater A5 and surface water (volume ratio 1:1) exhibited similar behavior under sunlight as wastewater: sunlight attenuated BCAN-FP faster than DCAN-FP, and reduced the overall cytotoxicity contributed by dihaloacetonitrile-FP, although the extent of reduction is generally smaller than that observed in wastewater alone. The behavior of

surface water was distinct: its DCAN-FP and BCAN-FP increased by 8% and 23%, respectively, after 36 h irradiation. This is consistent with a previous study reporting an increase in total HAN-FP of DCAN, DBAN, and TCAN from foliage leachate after fourteen days of ambient sunlight irradiation.⁵³ It is worth pointing out that while the DCAN-FP values of wastewater and surface water were within a factor of 2, the BCAN-FP of wastewater was 7 times higher than that of surface water, indicating much higher anticipated cytotoxicity from wastewater (Table S15). The strong association of BCAN-FP with wastewater, its relatively fast attenuation by sunlight, and the high toxicity of BCAN warrants further research.

3.2. Mechanistic Investigation of the Sunlight Effects on DCAN-FP and BCAN-FP

3.2.1. Change in the DCAN-FP and BCAN-FP of Model Precursor Solutions by Sunlight

Previous studies have carried out comprehensive surveys of DCAN precursors including amino acids and nucleic acids.^{10, 11} However, the concentrations of these precursors and their structural analogues in wastewater are often unknown. Therefore, in pursuing the mechanisms of the observed sunlight effects in this project, we opted to use a fluorescence EEM-directed approach. Although EEM does not provide quantitative/molecular-level details and information about non-fluorescing constituents, it is an easily accessible bulk analysis method and provides direction to what fluorescing moieties are associated with HAN formation. Regression analysis showed that the DCAN-FP and BCAN-FP of wastewater effluents correlated with the fluorescence intensity of tryptophan-like, tyrosine-like, and fulvic acid-like moieties in the EEM ($R^2 > 0.85$, Figure S17). Therefore, tryptophan, tyrosine, and Suwannee River fulvic acid were selected as model precursors. Tryptophan and tyrosine are also potent DCAN precursors as shown in the surveys,¹⁰ and are reactive under sunlight⁵⁴. Asparagine was selected as an additional precursor because of its extremely high yield of DCAN¹⁰ and the lack of any fluorescence signal. It should be

acknowledged that the concentrations of tryptophan, tyrosine, and asparagine, in the form of free amino acid, are low in wastewater,^{37, 39-41} but we believe that they bear relevance to the behavior of structurally similar compounds in terms of the change in DCAN-FP and BCAN-FP under sunlight and therefore can serve as model precursors in this preliminary investigation.

Figures 4a and 4b shows that sunlight photolysis of tryptophan and fulvic acid resulted in the decrease of their DCAN-FP and/or BCAN-FP, and BCAN-FP is overall more likely to show a decrease than DCAN-FP for each precursor. For tryptophan, the change in DCAN-FP by sunlight depended on irradiation time: DCAN-FP initially increased and then decreased; BCAN-FP, in contrast, decreased continuously. After 36 h, the irradiated tryptophan solution had similar changes in DCAN-FP and BCAN-FP, 18–31% lower than the non-irradiated solution. Our results are different from a previous study²⁵ showing that the DCAN-FP of tryptophan decreased continuously over 13 h of simulated sunlight irradiation, which may be explained by the higher light intensity (574 W/m^2) and lower precursor concentration (1.3 mg C/L) in this study compared with ours (320 W/m^2 , 5 mg C/L). Kynurenine and tryptamine, two major photoproducts of tryptophan upon 337 nm irradiation⁵⁵ and two DCAN precursors,^{11, 25} were monitored during tryptophan irradiation (Figure S18a). However, integrating the HAN-FP of these two intermediates (Figure S18b) and their concentrations cannot account for the change in the DCAN-FP or BCAN-FP of tryptophan solutions upon irradiation (Figure S18c, detailed discussion in Text S11), suggesting other intermediate(s) may play a more important role. For fulvic acid (Figure 4b), DCAN-FP remained unchanged, but BCAN-FP continuously decreased, reaching 38%–41% lower after 36 h irradiation. For tyrosine (Figure 4c) and asparagine (Figure 4d), DCAN-FP and BCAN-FP increased or did not change upon irradiation. BCAN-FP of asparagine was below detection limit, indicating it is not an important precursor for BCAN. The presence of bromide

(0.1 mg/L) during sunlight irradiation did not make a difference, with the only exception observed for the DCAN-FP of tryptophan, which started to decrease earlier in the presence of bromide.

3.2.2. Simulating Wastewater Effluent with Fulvic Acid and Tryptophan

To evaluate whether these model precursors can account for the behavior of wastewater under sunlight, tryptophan and/or fulvic acid were used to prepare synthetic effluents based on EEM results. Tyrosine was not used for three reasons: 1) wastewater samples generally have weak fluorescence intensity in the tyrosine-like region compared with the tryptophan- and fulvic acid-like regions in the EEM (Figure S19a); 2) the tyrosine-like region was not substantially removed by sunlight as the tryptophan- and fulvic acid-like regions (Figure S19b); 3) tyrosine did not show a decrease in BCAN-FP under sunlight as wastewater while tryptophan and fulvic acid did (Figure 4). The amount of tryptophan (50 $\mu\text{g C/L}$) and fulvic acid (2.5 mg C/L) used to constitute the synthetic wastewater effluent was selected such that they give rise to the same fluorescence intensity as effluent A5 in the tryptophan- and fulvic acid-like regions. Figure 3c shows the change in DCAN-FP and BCAN-FP by sunlight for the mixtures of surface water and different synthetic effluents (containing tryptophan, fulvic acid, or both). Synthetic effluents constituted by fulvic acid alone or by both fulvic acid and tryptophan closely approximated the behavior of the authentic wastewater effluent A5: DCAN-FP and BCAN-FP continuously decreased by sunlight. In contrast, the mixture of surface water and tryptophan-containing synthetic effluent behaved similar to surface water in terms of the increase in DCAN-FP under sunlight. These results overall suggest that fulvic acid can play an important role in the sunlight-induced change in HAN-FP from wastewater.

3.2.3. Reactivity of Fulvic acid as a Photosensitizer

Fulvic acid contains HAN precursors, as shown in previous studies^{56, 57} and our experiments (Table S16). Additionally, it can act as a photosensitizer for the transformation of pharmaceuticals and personal care products.⁵⁸⁻⁶¹ To differentiate these two roles of fulvic acid, we compared the change in HAN-FP by sunlight among three solutions: the surface water sample, a fulvic acid solution containing the same level of bromide, inorganic nitrogen species, and DOC as the surface water sample, and their 1:1 mixture (Figure 5). Prior to irradiation, the DCAN-FP and BCAN-FP of fulvic acid is less than one third of those of surface water. Upon sunlight irradiation, the mixture of surface water and fulvic acid exhibited 17% and 57% decrease in DCAN-FP and BCAN-FP, respectively, while no such change in HAN-FP was observed in fulvic acid alone. Additionally, the BCAN-FP of the mixture of surface water and fulvic acid decreased by an extent (0.080 $\mu\text{g}/\text{mg C}$) greater than the initial BCAN-FP of fulvic acid (0.058 $\mu\text{g}/\text{mg C}$). These results suggest that indirect photolysis, in which fulvic acid sensitized the decay of HAN precursors in surface water, may be the main contributor to the decrease in HAN-FP under sunlight for the mixture of surface water and wastewater effluents. Fulvic acid has been reported to sensitize the photodegradation of compounds that are known HAN precursors such as histidine, methionine, tyrosine, and tryptophan.⁵⁴

To further evaluate the role of fulvic acid as photosensitizer in wastewater effluents, the formation of excited triplet state organic matters in the effluents was measured by the probe compound 2,4,6-trimethylphenol, and compared with that in fulvic acid solutions that have the same concentration of fulvic acid-like moieties as the effluents. Figure S20 shows that 2,4,6-trimethylphenol decayed similarly in wastewater effluents and fulvic acid solutions, suggesting similar levels of excited triplet state organic matters were present in the samples. We also spiked fulvic acid into the solutions of different HAN precursors and observed that the decrease in HAN-

FP were promoted for tryptophan and asparagine (Figure 4 open squares), reinforcing the role of fulvic acid as a photosensitizer. For tryptophan, the decrease in DCAN-FP and BCAN-FP by sunlight irradiation in the presence of fulvic acid was respectively 16% and 25% more than that when tryptophan was irradiation alone. For asparagine, DCAN-FP decreased after sunlight irradiation in the presence of fulvic acid, in contrast to the increase in the absence of fulvic acid.

3.2.4. Reactivity of Tryptophan and Its UV Photoproducts as Photosensitizers

As mentioned above, for UV-disinfected effluents, increasing UV disinfection fluence did not affect the HAN-FP of wastewater effluents, but made it more likely for the effluents to feature a lower HAN-FP after sunlight irradiation (Figures 2 and S15a). The positive correlation between the UV disinfection fluence and the sunlight absorption ability of UV-irradiated effluent (Figure S16) suggests that UV can produce more sunlight-reactive constituents. To examine whether this trend can be replicated by model compounds, we conducted similar experiments on tryptophan and fulvic acid solutions. As shown in Figure S16, tryptophan solution exhibited a similar trend as effluent C6: samples irradiated by higher UV fluence showed a higher sunlight absorption ability; such trend was not observed in the fulvic acid solution. Additionally, FP experiments on tryptophan showed that UV did not affect its DCAN-FP, but the DCAN-FP after sunlight irradiation was lower for samples irradiated by higher fluence of UV (Figures S15b and S15c), similar to the observation for wastewater effluents (Figures 2 and S15a).

Tryptophan and its photoproducts are not only HAN precursors, but also photosensitizers under sunlight⁶²⁻⁶⁹. Because the extent of tryptophan decay by UV was small (<6% for up to 300 mJ/cm², Table S18), the difference made by UV to the change in HAN-FP under sunlight is likely attributed to tryptophan's UV photoproducts. Using benzoic acid and 2,4,6-trimethylphenol as

probes for hydroxyl radical ($\cdot\text{OH}$) and excited triplet state organic matters, respectively, we observed that the UV-irradiated tryptophan solutions generate significantly more excited triplet states (Figure S21). The decay of 2,4,6-trimethylphenol under sunlight was 7 times faster in 300 mJ/cm² UV-irradiated tryptophan solution than in the original tryptophan solution. In contrast, the degradation of benzoic acid was not different between these samples. We then tested the photosensitizing ability of tryptophan's UV products by spiking them into authentic surface water samples and examined the change in DCAN-FP under sunlight. As shown in Figure S22, the mixture of surface water and UV-irradiated tryptophan solution lost 20% of its DCAN-FP after 8 h sunlight irradiation, in contrast to the increase in DCAN-FP by sunlight in the mixture of surface water and tryptophan solution (not irradiated by UV), suggesting that the UV products of tryptophan indeed served as photosensitizers to degrade HAN precursors. Several UV products of tryptophan were reported to feature higher molar extinction coefficients than tryptophan^{55, 70-72} and act as sunlight photosensitizer.⁶²⁻⁶⁹ For example, kynurenine can form an excited triplet under 308 nm irradiation.⁶² However, kynurenine only accounted for 2% of the sunlight absorbance of the 150 mJ/cm² UV-irradiated tryptophan solution based on its molar extinction coefficient (Figure S23) and its concentration in the UV-irradiated tryptophan solution (Table S18). The other UV products of tryptophan such as *N*-formylkynurenine,^{65, 66} xanthurenic acid,^{67, 72} and kynurenic acid^{68, 69} that are reactive under sunlight but not monitored in this study may contribute more substantially to the photosensitizing behavior of UV-irradiated tryptophan solutions and should be considered in future research.

4. Environmental Implications

This study is one of the few to systematically evaluate the effects of sunlight on the HAN-FP of wastewater effluents as they travel downstream. We showed that by preferentially removing the formation potential of the more toxic BCAN over that of DCAN, sunlight can reduce the overall potential toxicity from the formation potential of dihaloacetonitriles, a group of N-DBPs shown to contribute higher risk to drinking water than other DBP groups.⁴ The reduction in potential cytotoxicity by 8 h of sunlight irradiation (equivalent to approximately 2–3 days under natural sunlight) ranges from 1% to 27%. The effects of sunlight also apply to mixtures of wastewater effluent and pristine surface water, which simulate the surface water immediately downstream of wastewater discharge. The comparison between chlorine- and UV-disinfected effluents suggests that the sunlight effects on HAN-FP were not affected by wastewater disinfection methods at environmentally relevant doses. However, higher UV disinfection fluences can make the effluents more susceptible to sunlight in losing their HAN-FP. By evaluating model compounds that are implicated by the fluorescence signals of authentic wastewater, we propose that both direct photolysis of HAN precursors (e.g., tryptophan and fulvic acid) and indirect photolysis (e.g., sensitized by fulvic acid and UV-products of tryptophan) contributed to the decrease in the HAN-FP of wastewater effluents by sunlight, with the latter being the more important mechanism (scheme in Figure S24). Future work is needed to continue to explore these pathways.

Our study enriches the knowledge on the roles of sunlight in transforming DBP formation potential of different waters.^{17, 24-26, 53} Overall, sunlight plays different roles for different sources of organic materials and different DBP precursors. For surface waters dominated by humic materials, sunlight can increase HAN-FP; for wastewater, however, sunlight can decrease HAN-FP. Sunlight can attenuate TCNM-FP for non-nitrified wastewater effluents but increase TCNM-

FP for wastewater effluents in the presence of nitrite. For both surface waters and wastewater effluents, sunlight increases THM-FP. Considering the varying toxicity of different DBPs, a comprehensive, toxicity-weighted evaluation is recommended for future studies.

Lastly, we would like to acknowledge two limitations of this study that should be addressed in the future. First, we prioritized the wastewater constituents that show fluorescence signals, taking advantage of the EEM technique to provide (semi-)quantitative insight into the behavior of wastewater effluents under sunlight. However, other non-fluorescing constituents should also be investigated in the future, especially those serving as HAN precursors (e.g., asparagine) that can be degraded by photosensitizers (e.g., fulvic acid). Second, we opted to use FP test in this study so that the results can be compared with previous surveys of wastewater HAN-FP and with the other studies on the sunlight effects of HAN-FP from wastewater effluent. However, future studies are needed to use drinking water relevant disinfection conditions, especially for investigating the relative formation of DCAN and BCAN.

Supporting Information

Additional details on experimental methods, and additional figures and tables for result and discussion.

Acknowledgements

The research was supported by the National Science Foundation (1805058 and 1652412). The authors thank the participating water and wastewater utilities for providing field samples. The authors also thank Dr. Richelle Allen-King for providing the instruments to analyze DOC, TN, nitrite, and nitrate.

501 **Declaration of Competing Interests**

502 The authors declare that they have no known competing financial interests or personal
503 relationships that could have appeared to influence the work reported in this paper.

References

1. McGuire, M. J.; McLain, J. L.; Obolensky, A., *Information Collection Rule Data Analysis*. AWWA Research Foundation and American Water Works Association: Denver, CO, **2002**.
2. Krasner, S. W.; Westerhoff, P.; Chen, B. Y.; Rittmann, B. E.; Nam, S. N.; Amy, G., Impact of wastewater treatment processes on organic carbon, organic nitrogen, and DBP precursors in effluent organic matter. *Environ. Sci. Technol.* **2009**, *43* (8), 2911-2918.
3. Wagner, E. D.; Plewa, M. J., CHO cell cytotoxicity and genotoxicity analyses of disinfection by-products: An updated review. *J. Environ. Sci.-China* **2017**, *58*, 64-76.
4. Plewa, M. J.; Wagner, E. D.; Richardson, S. D., TIC-Tox: A preliminary discussion on identifying the forcing agents of DBP-mediated toxicity of disinfected water. *J. Environ. Sci.-China* **2017**, *58*, 208-216.
5. Phatthalung, W. N.; Musikavong, C., Emerging disinfection by-products' formation potential in raw water, wastewater, and treated wastewater in Thailand. *J. Environ. Sci. Health, Part A* **2019**, *54* (8), 745-758.
6. Krasner, S. W.; Westerhoff, P.; Chen, B.; Amy, G.; Nam, S.; Chowdhury, Z.; Sinha, S.; Rittmann, B. *Contribution of Wastewater to DBP Formation*; AwwaRF: Denver, Colorado, 2008.
7. Chen, B.; Westerhoff, P., Predicting disinfection by-product formation potential in water. *Water Res.* **2010**, *44* (13), 3755-3762.
8. Lee, W.; Westerhoff, P.; Croué, J.-P., Dissolved organic nitrogen as a precursor for chloroform, dichloroacetonitrile, *N*-nitrosodimethylamine, and trichloronitromethane. *Environ. Sci. Technol.* **2007**, *41* (15), 5485-5490.
9. Hu, H. Y.; Du, Y.; Wu, Q. Y.; Zhao, X.; Tang, X.; Chen, Z., Differences in dissolved organic matter between reclaimed water source and drinking water source. *Sci. Total Environ.* **2016**, *551*, 133-142.
10. Yang, X.; Shen, Q. Q.; Guo, W. H.; Peng, J. F.; Liang, Y. M., Precursors and nitrogen origins of trichloronitromethane and dichloroacetonitrile during chlorination/chloramination. *Chemosphere* **2012**, *88* (1), 25-32.
11. Ueno, H.; Moto, T.; Sayato, Y.; Nakamuro, K., Disinfection by-products in the chlorination of organic nitrogen compounds: By-products from kynurenine. *Chemosphere* **1996**, *33* (8), 1425-1433.
12. Obolensky, A.; Singer, P. C., Halogen substitution patterns among disinfection byproducts in the information collection rule database. *Environ. Sci. Technol.* **2005**, *39* (8), 2719-2730.
13. Jia, A. Y.; Wu, C. D.; Duan, Y., Precursors and factors affecting formation of haloacetonitriles and chloropicrin during chlor(am)ination of nitrogenous organic compounds in drinking water. *J. Hazard. Mater.* **2016**, *308*, 411-418.
14. Huang, H.; Chen, B.-Y.; Zhu, Z.-R., Formation and speciation of haloacetamides and haloacetonitriles for chlorination, chloramination, and chlorination followed by chloramination. *Chemosphere* **2017**, *166*, 126-134.
15. Xue, C. H.; Wang, Q.; Chu, W. H.; Templeton, M. R., The impact of changes in source water quality on trihalomethane and haloacetonitrile formation in chlorinated drinking water. *Chemosphere* **2014**, *117*, 251-255.

16. Hladik, M. L.; Focazio, M. J.; Engle, M., Discharges of produced waters from oil and gas extraction via wastewater treatment plants are sources of disinfection by-products to receiving streams. *Sci. Total Environ.* **2014**, 466-467, 1085-1093.
17. Du, Y.; Zhang, X.; Li, C.; Wu, Q. Y.; Huang, H.; Hu, H. Y., Transformation of DON in reclaimed water under solar light irradiation leads to decreased haloacetamide formation potential during chloramination. *J. Hazard. Mater.* **2017**, 340, 319-325.
18. Yang, X. F.; Meng, F. G.; Huang, G. C.; Sun, L.; Lin, Z., Sunlight-induced changes in chromophores and fluorophores of wastewater-derived organic matter in receiving waters - The role of salinity. *Water Res.* **2014**, 62, 281-292.
19. Wu, Q. Y.; Li, C.; Wang, W. L.; He, T.; Hu, H. Y.; Du, Y.; Wang, T., Removal of fluorescence and ultraviolet absorbance of dissolved organic matter in reclaimed water by solar light. *J. Environ. Sci.-China* **2016**, 43, 118-127.
20. McKay, G.; Korak, J. A.; Erickson, P. R.; Latch, D. E.; McNeill, K.; Rosario-Ortiz, F. L., The case against charge transfer interactions in dissolved organic matter photophysics. *Environ. Sci. Technol.* **2018**, 52 (2), 406-414.
21. Rosario-Ortiz, F. L.; Canonica, S., Probe compounds to assess the photochemical activity of dissolved organic matter. *Environ. Sci. Technol.* **2016**, 50 (23), 12532-12547.
22. Silva, M. P.; Lastre-Acosta, A. M.; Mostafa, S.; McKay, G.; Linden, K. G.; Rosario-Ortiz, F. L.; Teixeira, A. C. S. C., Photochemical generation of reactive intermediates from urban-waste bio-organic substances under UV and solar irradiation. *Environ. Sci. Pollut. R.* **2017**, 24 (22), 18470-18478.
23. Zhang, X.; Yang, C.-W.; Li, J.; Yuan, L.; Sheng, G.-P., Spectroscopic insights into photochemical transformation of effluent organic matter from biological wastewater treatment plants. *Sci. Total Environ.* **2019**, 649, 1260-1268.
24. Xu, J.; Kralles, Z. T.; Dai, N., Effects of Sunlight on the Trichloronitromethane Formation Potential of Wastewater Effluents: Dependence on Nitrite Concentration. *Environ. Sci. Technol.* **2019**, 53 (8), 4285-4294.
25. Wu, Q. Y.; Li, C.; Du, Y.; Wang, W. L.; Huang, H.; Hu, H. Y., Elimination of disinfection byproduct formation potential in reclaimed water during solar light irradiation. *Water Res.* **2016**, 95, 260-267.
26. Wu, J.; Ye, J.; Peng, H. L.; Wu, M. R.; Shi, W. W.; Liang, Y. M.; Liu, W., Solar photolysis of soluble microbial products as precursors of disinfection by-products in surface water. *Chemosphere* **2018**, 201, 66-76.
27. Antoniou, C. V.; Koukouraki, E. E.; Diamadopoulos, E., Determination of chlorinated volatile organic compounds in water and municipal wastewater using headspace–solid phase microextraction–gas chromatography. *J. Chromatogr. A* **2006**, 1132 (1), 310-314.
28. Doederer, K.; Gernjak, W.; Weinberg, H. S.; Farré, M. J., Factors affecting the formation of disinfection by-products during chlorination and chloramination of secondary effluent for the production of high quality recycled water. *Water Res.* **2014**, 48, 218-228.
29. Liu, W.; Zhang, Z.; Yang, X.; Xu, Y.; Liang, Y., Effects of UV irradiation and UV/chlorine co-exposure on natural organic matter in water. *Sci. Total Environ.* **2012**, 414, 576-584.
30. Hambly, A. C.; Henderson, R. K.; Storey, M. V.; Baker, A.; Stuetz, R. M.; Khan, S. J., Fluorescence monitoring at a recycled water treatment plant and associated dual distribution system – Implications for cross-connection detection. *Water Res.* **2010**, 44 (18), 5323-5333.

31. Rice, J.; Westerhoff, P., Spatial and temporal variation in de facto wastewater reuse in drinking water systems across the U.S.A. *Environ. Sci. Technol.* **2015**, *49* (2), 982-989.
32. Su, L.; Sivey, J. D.; Dai, N., Emerging investigator series: sunlight photolysis of 2,4-D herbicides in systems simulating leaf surfaces. *Environ. Sci.-Proc. Imp.* **2018**, *20* (8), 1123-1135.
33. Westerhoff, P.; Chen, W.; Esparza, M., Fluorescence analysis of a standard fulvic acid and tertiary treated wastewater. *J. Environ. Qual.* **2001**, *30* (6), 2037-2046.
34. Murphy, K. R.; Stedmon, C. A.; Graeber, D.; Bro, R., Fluorescence spectroscopy and multi-way techniques. PARAFAC. *Anal. Methods* **2013**, *5* (23), 6557-6566.
35. Pucher, M.; Graeber, D.; Preiner, S.; Pinto, R., *staRdom: PARAFAC Analysis of EEMs from DOM*, 1.0.14; 2019.
36. Chen, W.; Westerhoff, P.; Leenheer, J. A.; Booksh, K., Fluorescence excitation emission matrix regional integration to quantify spectra for dissolved organic matter. *Environ. Sci. Technol.* **2003**, *37* (24), 5701-5710.
37. Ma, H.; Allen, H. E.; Yin, Y., Characterization of isolated fractions of dissolved organic matter from natural waters and a wastewater effluent. *Water Res.* **2001**, *35* (4), 985-996.
38. Sierra, M. M. D.; Giovanela, M.; Parlanti, E.; Soriano-Sierra, E. J., Fluorescence fingerprint of fulvic and humic acids from varied origins as viewed by single-scan and excitation/emission matrix techniques. *Chemosphere* **2005**, *58* (6), 715-733.
39. Confer, D. R.; Logan, B. E.; Aiken, B. S.; Kirchman, D. L., Measurement of dissolved free and combined amino acids in unconcentrated wastewaters using high performance liquid chromatography. *Water Environ. Res.* **1995**, *67* (1), 118-125.
40. Rebhun, M.; Manka, J., Classification of organics in secondary effluents. *Environ. Sci. Technol.* **1971**, *5* (7), 606-609.
41. Fujita, Y.; Ding, W.-H.; Reinhard, M., Identification of wastewater dissolved organic carbon characteristics in reclaimed wastewater and recharged groundwater. *Water Environ. Res.* **1996**, *68* (5), 867-876.
42. *U.S. Wastewater Treatment Factsheet*; Center for Sustainable Systems, University of Michigan, 2018.
43. *Wastewater Technology Factsheet: Chlorine Disinfection*; U.S. EPA, 1999.
44. Nguyen, T.; Westerhoff, P.; Furlong, E. T.; Kolpin, D. W.; Batt, A. L.; Mash, H. E.; Schenck, K. M.; Boone, J. S.; Rice, J.; Glassmeyer, S. T., Modeled de facto reuse and contaminants of emerging concern in drinking water source waters. *J. Am. Water Works Ass.* **2018**, *110* (4), E2-E18.
45. Schwarzenbach, R. P.; Gschwend, P. M.; Imboden, D. M., *Environmental Organic Chemistry*. 2nd ed.; Wiley: Hoboken, NJ, 2003.
46. Yu, Y.; Reckhow, D. A., Kinetic Analysis of Haloacetonitrile Stability in Drinking Waters. *Environ. Sci. Technol.* **2015**, *49* (18), 11028-11036.
47. Tan, Y.; Lin, T.; Jiang, F.; Dong, J.; Chen, W.; Zhou, D., The shadow of dichloroacetonitrile (DCAN), a typical nitrogenous disinfection by-product (N-DBP), in the waterworks and its backwash water reuse. *Chemosphere* **2017**, *181*, 569-578.
48. Hong, H.; Song, Q.; Mazumder, A.; Luo, Q.; Chen, J.; Lin, H.; Yu, H.; Shen, L.; Liang, Y., Using regression models to evaluate the formation of trihalomethanes and haloacetonitriles via chlorination of source water with low SUVA values in the Yangtze River Delta region, China. *Environ. Geochem. Health* **2016**, *38* (6), 1303-1312.

49. Inamdar, S.; Finger, N.; Singh, S.; Mitchell, M.; Levina, D.; Bais, H.; Scott, D.; McHale, P., Dissolved organic matter (DOM) concentration and quality in a forested mid-Atlantic watershed, USA. *Biogeochemistry* **2012**, *108* (1-3), 55-76.
50. Nam, S.-N., Characterization and differentiation of wastewater effluent organic matter (EfOM) versus drinking water natural organic matter (NOM): implications for indirect potable reuse. University of Colorado at Boulder, **2011**.
51. Tang, H. L.; Chen, Y.-C.; Regan, J. M.; Xie, Y. F., Disinfection by-product formation potentials in wastewater effluents and their reductions in a wastewater treatment plant. *J. Environ. Monit.* **2012**, *14* (6), 1515-1522.
52. Huang, H.; Wu, Q.-Y.; Tang, X.; Jiang, R.; Hu, H.-Y., Formation of haloacetonitriles and haloacetamides and their precursors during chlorination of secondary effluents. *Chemosphere* **2016**, *144*, 297-303.
53. Chow, A. T.; Díaz, F. J.; Wong, K.-H.; O'Geen, A. T.; Dahlgren, R. A.; Wong, P.-K., Photochemical and bacterial transformations of disinfection by-product precursors in water. *J. Environ. Qual.* **2013**, *42* (5), 1589-1595.
54. Boreen, A. L.; Edhlund, B. L.; Cotner, J. B.; McNeill, K., Indirect photodegradation of dissolved free amino acids: The contribution of singlet oxygen and the differential reactivity of DOM from various sources. *Environ. Sci. Technol.* **2008**, *42* (15), 5492-5498.
55. Borkman, R. F.; Hibbard, L. B.; Dillon, J., The photolysis of tryptophan with 337.1 nm laser radiation. *Photochem. Photobiol.* **1986**, *43* (1), 13-19.
56. Reckhow, D. A.; Singer, P. C., Chlorination by-products in drinking waters: From formation potentials to finished water concentrations. *J. Am. Water Works Ass.* **1990**, *82* (4), 173-180.
57. Oliver, B. G., Dihaloacetonitriles in drinking water: algae and fulvic acid as precursors. *Environ. Sci. Technol.* **1983**, *17* (2), 80-83.
58. Chen, Y.; Li, H.; Wang, Z.; Li, H.; Tao, T.; Zuo, Y., Photodegradation of selected β -blockers in aqueous fulvic acid solutions: Kinetics, mechanism, and product analysis. *Water Res.* **2012**, *46* (9), 2965-2972.
59. Guerard, J. J.; Miller, P. L.; Trouts, T. D.; Chin, Y.-P., The role of fulvic acid composition in the photosensitized degradation of aquatic contaminants. *Aquat. Sci.* **2009**, *71* (2), 160-169.
60. Makunina, M. P.; Pozdnyakov, I. P.; Chen, Y.; Grivin, V. P.; Bazhin, N. M.; Plyusnin, V. F., Mechanistic study of fulvic acid assisted propranolol photodegradation in aqueous solution. *Chemosphere* **2015**, *119*, 1406-1410.
61. Jacobs, L. E.; Fimmen, R. L.; Chin, Y.-P.; Mash, H. E.; Weavers, L. K., Fulvic acid mediated photolysis of ibuprofen in water. *Water Res.* **2011**, *45* (15), 4449-4458.
62. Tsentalovich, Y. P.; Snytnikova, O. A.; Sherin, P. S.; Forbes, M. D. E., Photochemistry of kynurenine, a tryptophan metabolite: properties of the triplet state. *J. Phys. Chem. A* **2005**, *109* (16), 3565-3568.
63. Grossweiner, L. I., Photochemistry of proteins: a review. *Curr. Eye Res.* **1984**, *3* (1), 137-144.
64. Kerwin, B. A.; Remmele, R. L., Jr., Protect from light: photodegradation and protein biologics. *J. Pharm. Sci.* **2007**, *96* (6), 1468-1479.
65. Walrant, P.; Santus, R.; Grossweiner, L., Photosensitizing properties of *N*-formylkynurenine. *Photochem. Photobiol.* **1975**, *22* (1- 2), 63-65.

- 682 66. Schäfer, K.; Goddinger, D.; Höcker, H., Photodegradation of tryptophan in wool. *J. Soc.*
683 *Dyers Colour.* **1997**, *113* (12), 350-355.
- 684 67. Roberts, J. E.; Wishart, J. F.; Martinez, L.; Chignell, C. F., Photochemical studies on
685 xanthurenic acid. *Photochem. Photobiol.* **2000**, *72* (4), 467-471.
- 686 68. Pileni, M. P.; Giraud, M.; Santus, R., Kynurenic acid – II. Photosensitizing properties.
687 *Photochem. Photobiol.* **1979**, *30* (2), 257-261.
- 688 69. Catalfo, A.; Bracchitta, G.; De Guidi, G., Role of aromatic amino acid tryptophan UVA-
689 photoproducts in the determination of drug photosensitization mechanism: a comparison between
690 methylene blue and naproxen. *Photoch. Photobio. Sci.* **2009**, *8* (10), 1467-1475.
- 691 70. Pileni, M. P.; Walrant, P.; Santus, R., Electronic properties of *N*-formylkynurenine and
692 related compounds. *J. Phys. Chem.* **1976**, *80* (16), 1804-1809.
- 693 71. Lesniak, W. G.; Jyoti, A.; Mishra, M. K.; Louissaint, N.; Romero, R.; Chugani, D. C.;
694 Kannan, S.; Kannan, R. M., Concurrent quantification of tryptophan and its major metabolites.
695 *Anal. Biochem.* **2013**, *443* (2), 222-231.
- 696 72. Slawiński, J.; Elbanowski, M.; Slawińska, D., Spectral characteristics and mechanism of
697 chemiluminescence from tryptophan solutions induced by UV-irradiation. *Photochem.*
698 *Photobiol.* **1980**, *32* (2), 253-260.

Figure 1. Change in the DCAN-FP and BCAN-FP of (a) two non-nitrified (A4 and B3) and two nitrified (C5 and D2) effluent samples over 36 h irradiation; change in the DCAN-FP and BCAN-FP of (b) sixteen chlorine-disinfected and (d) thirteen UV-disinfected effluent samples after 8 h irradiation; change in the calculated cytotoxicity contributed by dihaloacetonitrile-FP of (c) sixteen chlorine-disinfected and (e) thirteen UV-disinfected effluent samples after 8 h irradiation. Details of the experimental procedure are described in section 2.3. The UV incident fluence for (d) and (e) was 12 mJ/cm². Error bars represent the standard deviation from duplicate experiments. The fitting curves in (a) correspond to pseudo-first order kinetics. Tables S6 and S12 show the values of DOC-normalized DCAN- or BCAN-FP and the calculated cytotoxicity for each sample.

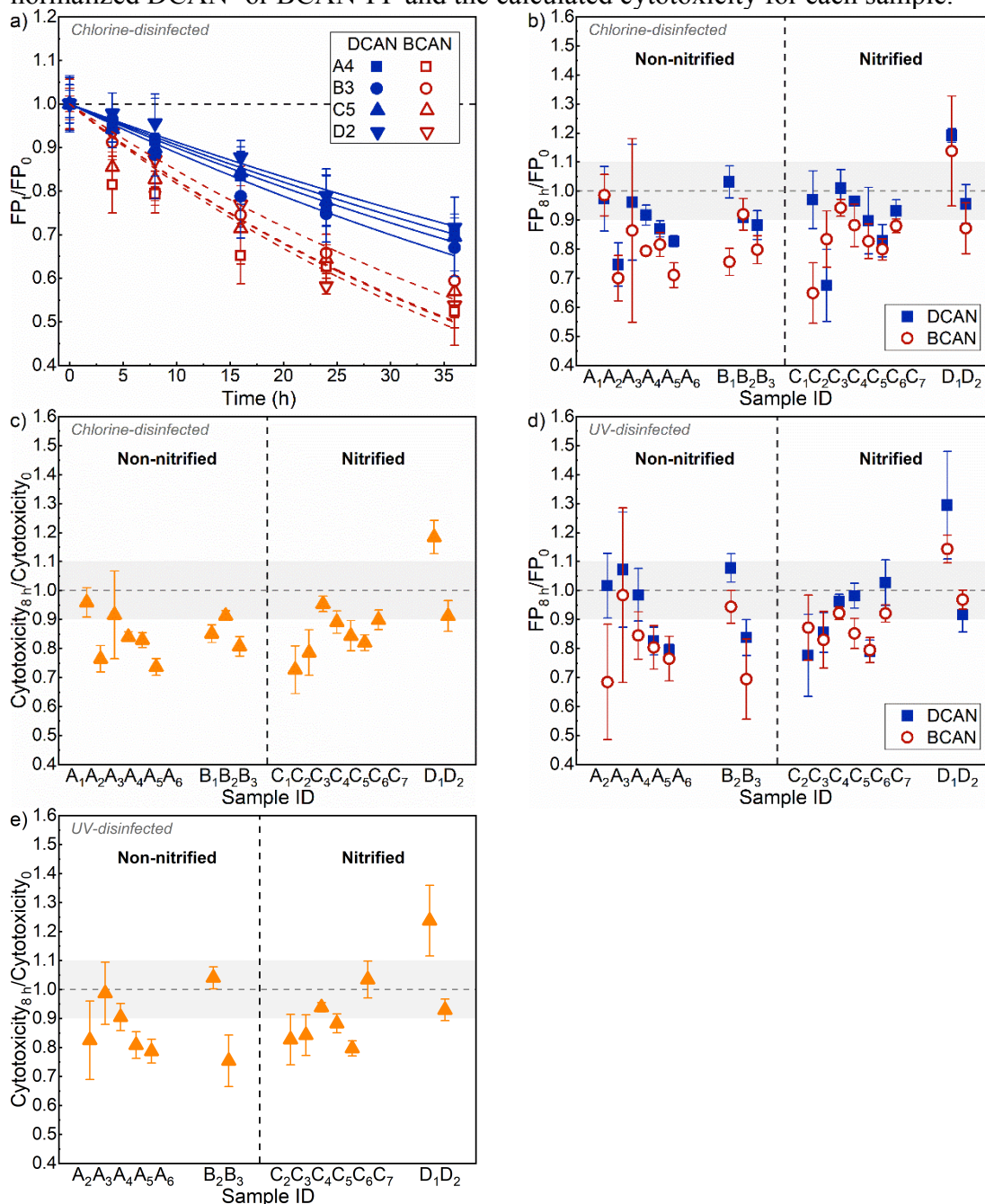


Figure 2. Change in DCAN-FP and BCAN-FP after 8 h simulated sunlight irradiation for wastewater samples disinfected by different UV fluences. A4 and B2 were non-nitrified effluents; C4 and D1 were nitrified effluents. Details of the experimental procedure are described in section 2.3. Error bars represent the standard deviation from duplicate experiments. Table S12 shows the values of DOC-normalized DCAN- or BCAN-FP for each sample.

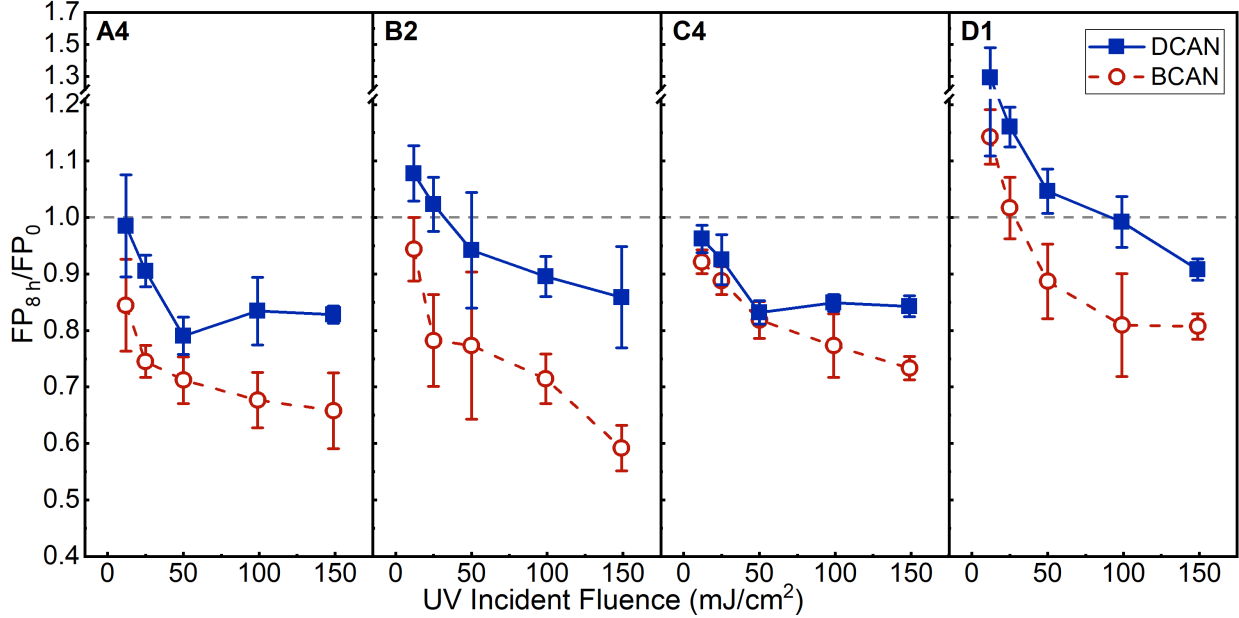


Figure 3. Change in (a) DCAN-FP and BCAN-FP and (b) calculated cytotoxicity from dihaloacetonitrile-FP by sunlight for chlorine-disinfected effluent A5, surface water, and their mixture (volume ratio 1:1); (c) change in DCAN-FP and BCAN-FP by sunlight for mixtures of SW and synthetic wastewater solutions (volume ratio 1:1) containing tryptophan, fulvic acid, or both tryptophan and fulvic acid. The preparation of synthetic wastewater is described in Text S6. Error bars represent the standard deviation from duplicate experiments. Table S15 shows the values of DOC-normalized DCAN- or BCAN-FP for each sample. Abbreviations: SW, surface water; WW, wastewater; Trp, tryptophan; FA, fulvic acid.

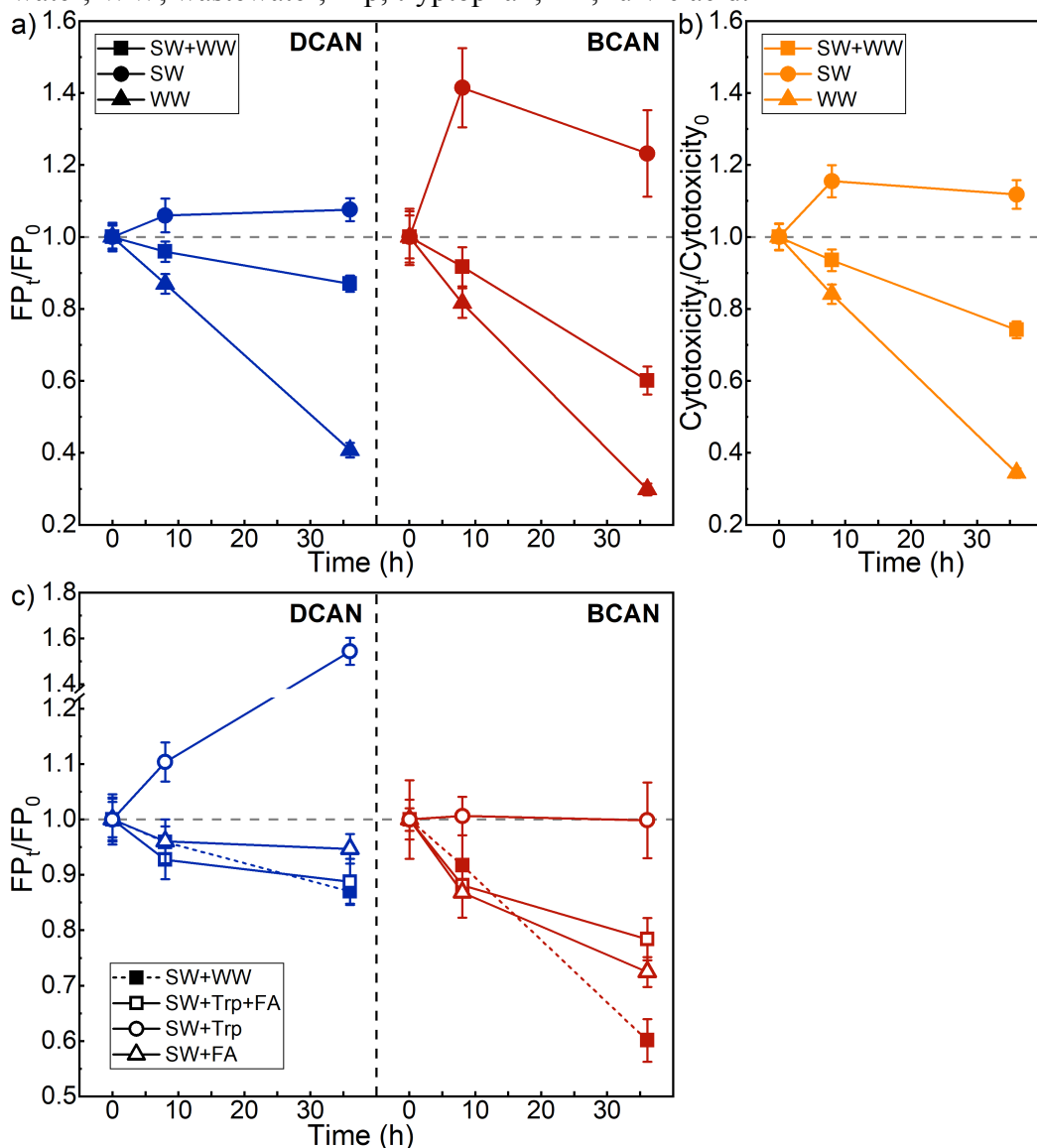


Figure 4. Change in DCAN-FP and BCAN-FP by simulated sunlight for (a) tryptophan, (b) fulvic acid, (c) tyrosine, and (d) asparagine solutions. The solutions were buffered at pH 7.2 by 5 mM phosphate and contained 5 mg C/L precursor compound. Bromide (0.1 mg/L) was not spiked (“No Br⁻”), or spiked before (“+Br⁻ before”) or after (“+Br⁻ after”) sunlight irradiation. Fulvic acid (2.5 mg C/L) was spiked (“+FA”) in selected tryptophan, tyrosine, and asparagine solutions. All samples were irradiated under simulated sunlight (320 W/m²) over 36 h and then subject to FP test. Error bars represent the standard deviation from duplicate experiments. Table S16 shows the values of DOC-normalized DCAN- or BCAN-FP for each sample. BCAN-FP of asparagine was below detection limit.

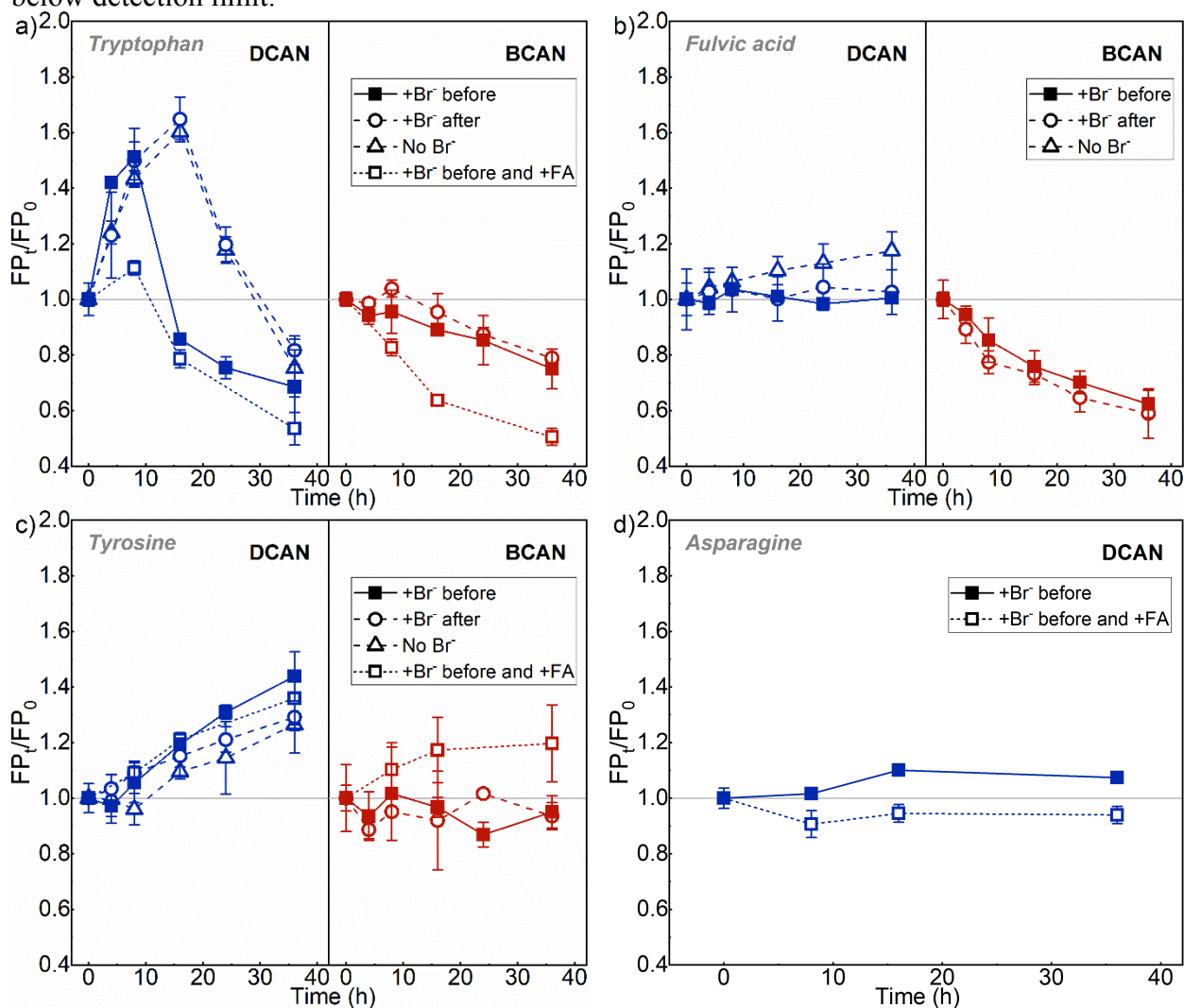


Figure 5. Change in DCAN-FP and BCAN-FP by sunlight irradiation for a surface water sample, a fulvic acid solution, and a mixture of surface water and fulvic acid solution (volume ratio 1:1). The fulvic acid solution was prepared with the same bromide, inorganic nitrogen, and DOC concentrations as SW and buffered by 5 mM phosphate at pH 7.2. Samples were irradiated under simulated sunlight (320 W/m²) over 36 h and then subject to FP test. Error bars represent the standard deviation from duplicate experiments. Table S17 shows the values of DOC-normalized DCAN- or BCAN-FP for each sample. Abbreviations: SW, surface water; FA, fulvic acid.

